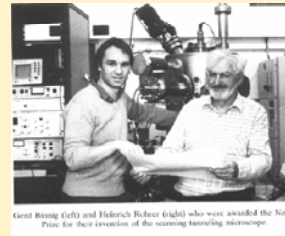


ATOMIC FORCE MICROSCOPY: IMAGING THE EFFECT OF METAL ION COMPLEXES ON DNA AND PROTEINS

Prof. Dr. Virtudes Moreno Martínez
 Departamento de Química Inorgánica
 Universidad de Barcelona
 Martí Franqués 1-11, 08028-Barcelona (España)
 Tlf. 0034 934021274
virtudes.moreno@qi.ub.es

Introduction

Atomic Force Microscope (AFM) is part of a large family of Scanning Probe Microscopes (SPM).



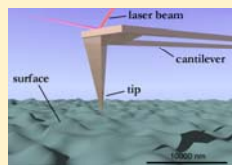
* The First SPM was invented in 1981 by Gerd Binnig and Heinrich Rohrer.

* Early SPM models acquired images by detecting the difference in electrical potential between two objects on the slide.

* AFM, developed in 1986, generates images based on the attraction and repulsion forces between the scanning tip and the objects on the slide.

Principles of Atomic Force Microscopy

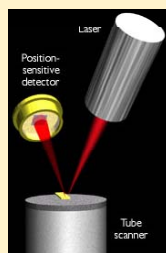
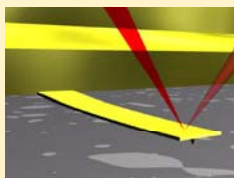
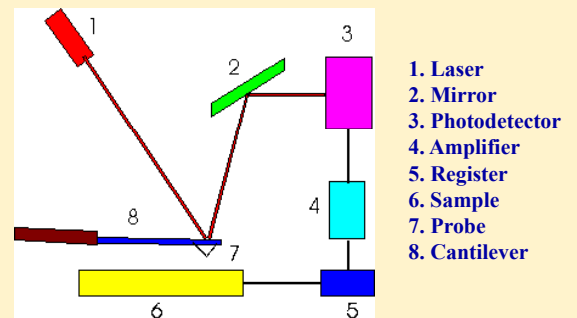
* Images in AFM are acquired by scanning the surface of the sample with a sharp tip.



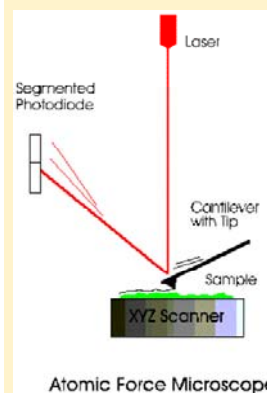
* The tip is located at the free end of a flexible cantilever.

* The cantilever movements are detected by a laser beam that is reflected of the back of the cantilever to a photodiode.

AFM Scheme



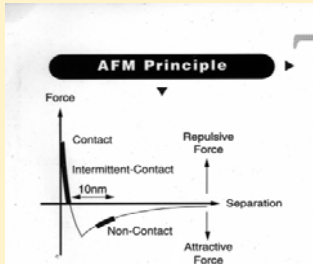
(Left) a cantilever touching a sample; (right) the optical lever. Scale drawing; the tube scanner measures 24 mm in diameter, while the cantilever is 100 μm long.



* Forces between the tip and the sample cause the cantilever to deflect

* The photodiode relays the information to the computer which in turn generates a topographical image of the sample

AFM Operation

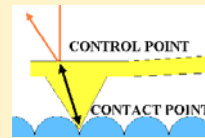
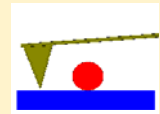


- Contact Mode
- Non Contact Mode
- Intermittent Contact Mode (Tapping)

The AFM can be used in a variety of environments: air, UHV (ultra high vacuum) and under liquids

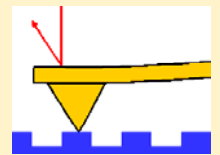
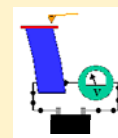
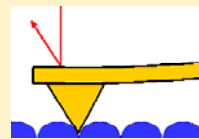


TIP



The sharp tip is dragged across a sample surface

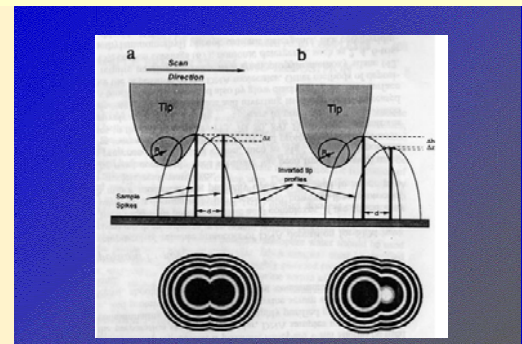
Now, the sample is moving under the AFM tip



Resolution in AFM

- AFM does not use lenses to generate images.
- Resolution in AFM is dependent on:
 - The sharpness of the tip.
 - The distance between the objects to be resolved.
 - The height of the two objects to be resolved.

Resolution in AFM



A schematic diagram showing the factors that affect resolution in AFM

Sample Preparation

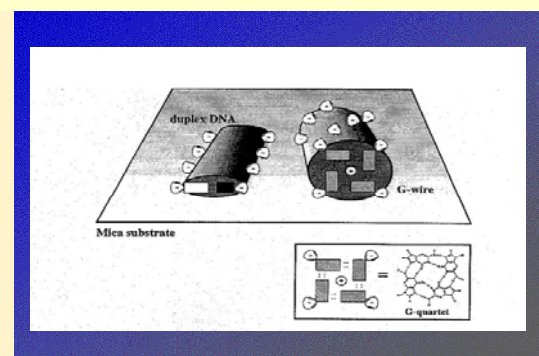
Deposition Buffer containing a divalent cation.

Proper concentration of reactants

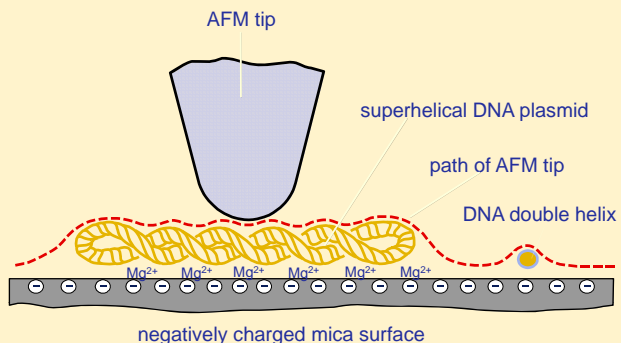
Flat substrate:

1. Plain mica
2. Aminopropyltrimethoxy saline (APTES) mica
3. Glow discharged mica

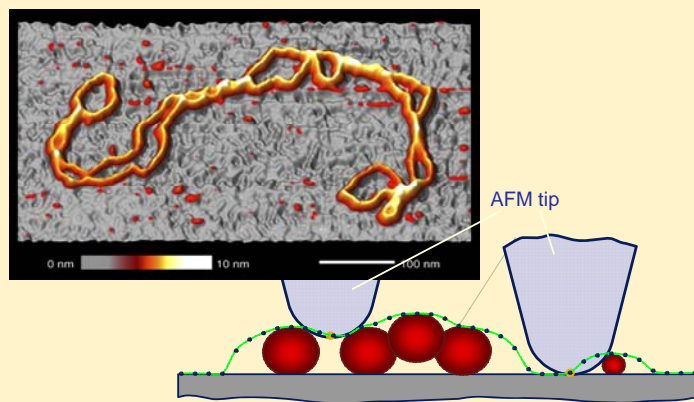
A drawing showing the attachment of the DNA molecules to the mica substrate.



movement of the AFM tip along the sample

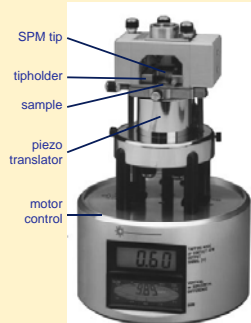
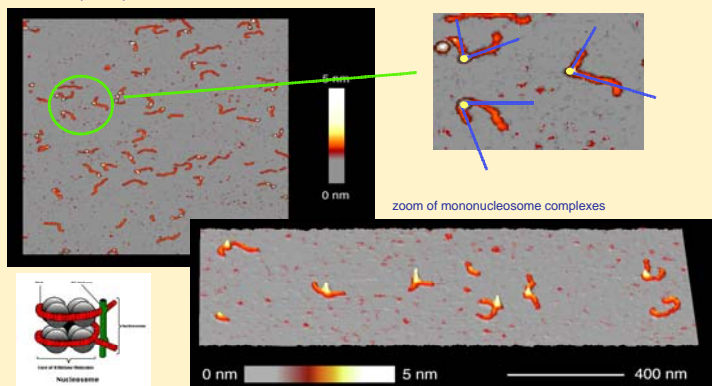


AFM image of a 6.8 kb superhelical plasmid



AFM image of a nucleosome on a 614 base pair DNA

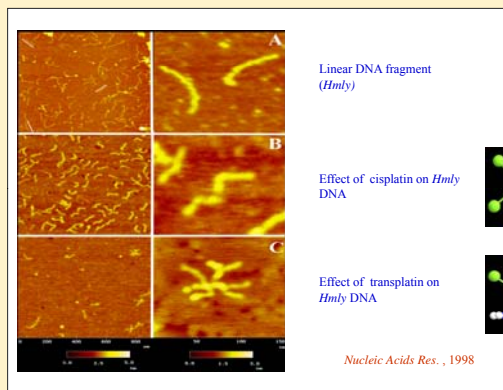
2 μm x 2 μm overview scan



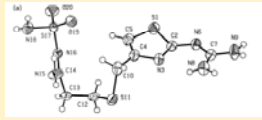
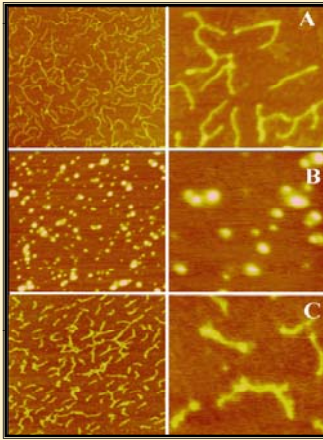
In the picture, one of the most recent SPM Microscope from Digital Instruments is shown. This is the Instrument available in the Laboratories of the Serveis Científics-Tècnics of our University.

Probing the modifications in linear DNA and circular plasmid DNA caused by a variety of metal-complexes by Tapping Mode AFM.

The experiments were always done in air, on peeled mica and low humidity.



Famotidine



Pd-Famotidine

Pt-Famotidine

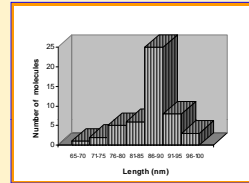
Effect of Famotidine and their Pd(II) and Pt(II) complexes on *Hmly*

Nucleic Acids Research, 1998

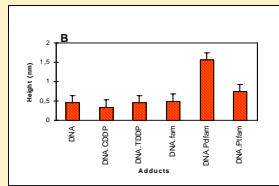
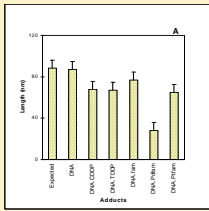
Dimensions of DNA and several DNA-complex adducts. (Standard deviation errors are ±1).

Adducts	Length (nm)	height (nm)	width(nm)
DNA	87±6.5	0.45±0.06	10.2±0.7
DNA.CDDP	68±9.0	0.38±0.15	13.1±0.6
DNA.TDDP	67±7.2	0.45±0.07	16.4±2.1
DNA.fam	77±7.9	0.50±0.07	14.6±0.6
DNA.PdFam	28±20	1.57±0.38	**
DNA.PtFam	64±12	0.74±0.16	22.2±3.5

** measurement of length and width are equivalents due to its oval shape.



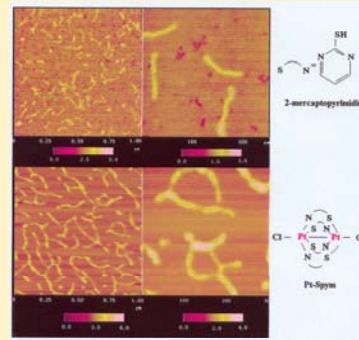
Quantitative analysis of the TMAFM images. Histogram of the mean lengths of the free *Hmly* fragments. The apparent average length ± standard deviation was 87±6.5 nm for the 50% of the measured population.



Graphical representation (error bars) of the standard deviation of the mean values for the different DNA-complexes adducts imaged.

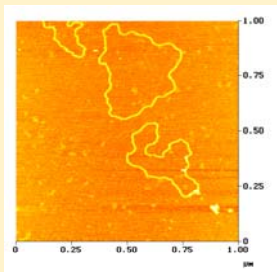
(A) Comparison between the different apparent mean values and the expected length for DNA.

(B) Comparison between the apparent mean values and the expected height for DNA.

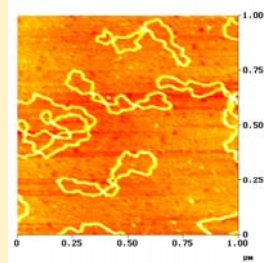


Effect of 2-mercaptopyrimidine and a dinuclear Pt(III) complex with this molecule on *Hmly*

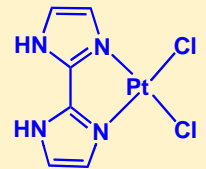
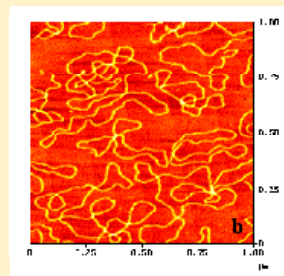
Nucleic Acids Research, 1998
J.Inorg.Biochem., 1999



Plasmid DNA pBR322

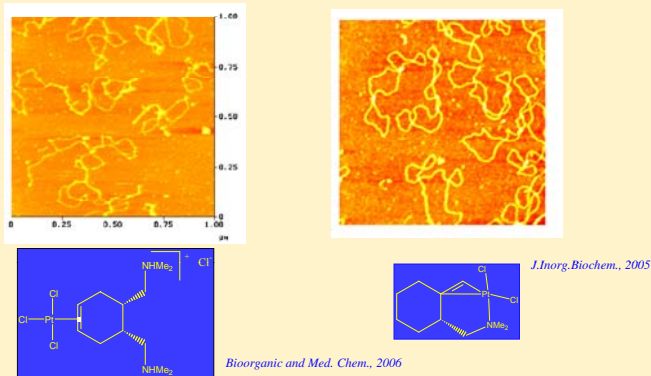


DNA pBR322 + cisplatin

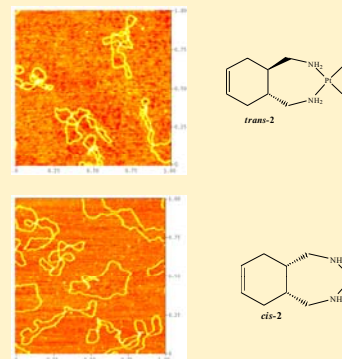


Modifications caused by an analogue to cisplatin on the same DNA

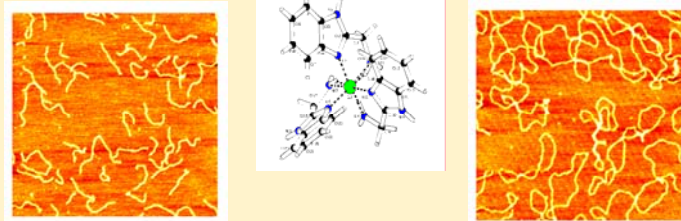
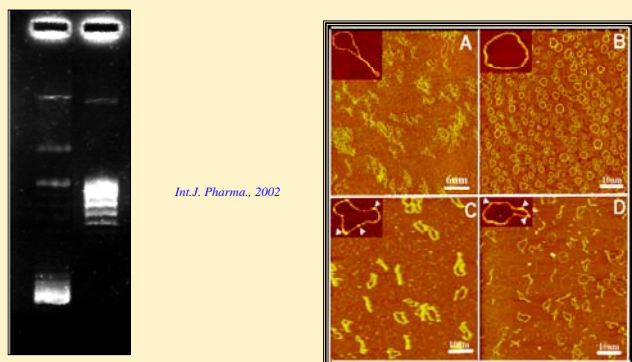
Comparison between modifications caused on pBR322 by two π platinum, cationic and neutral, complexes



Modifications caused on pBR322 plasmid DNA by the two diastereoisomers of the picture show the stronger interaction of the *trans* Pt diamine complex.

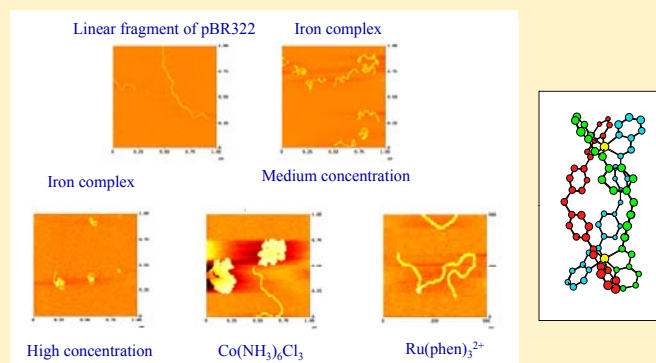
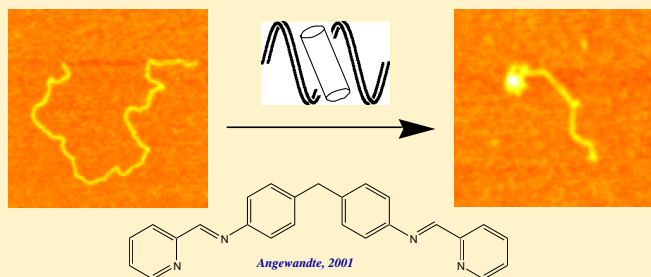


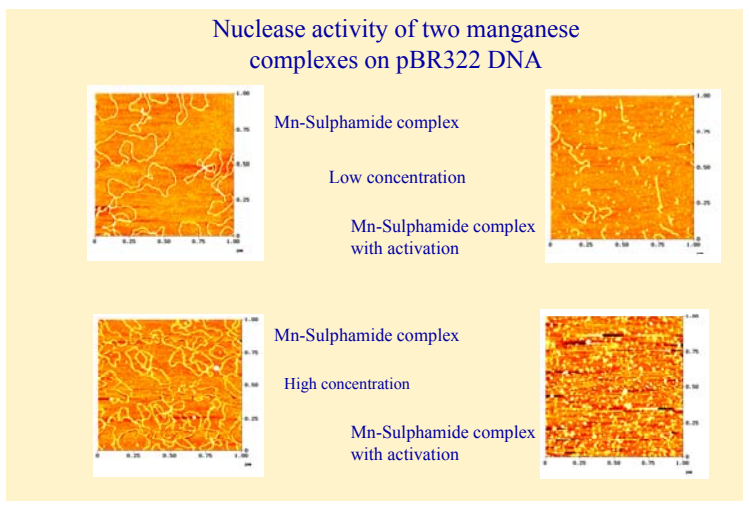
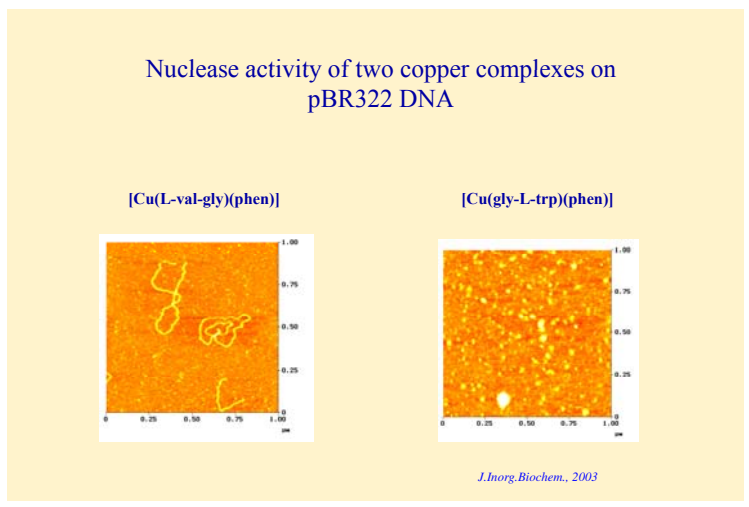
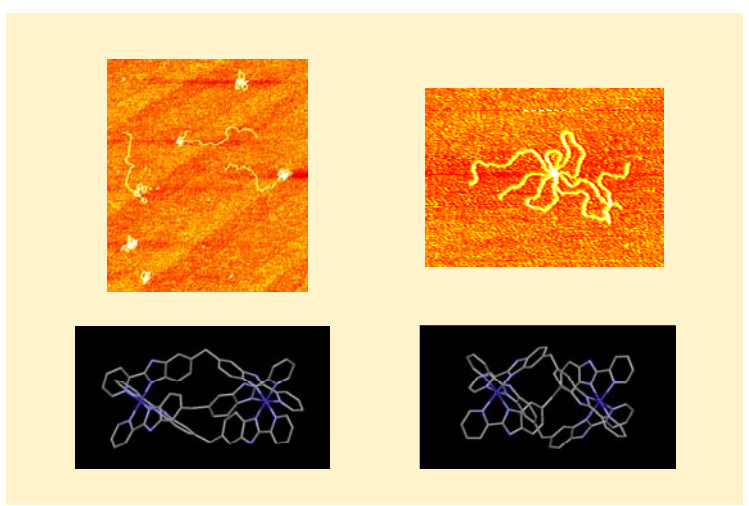
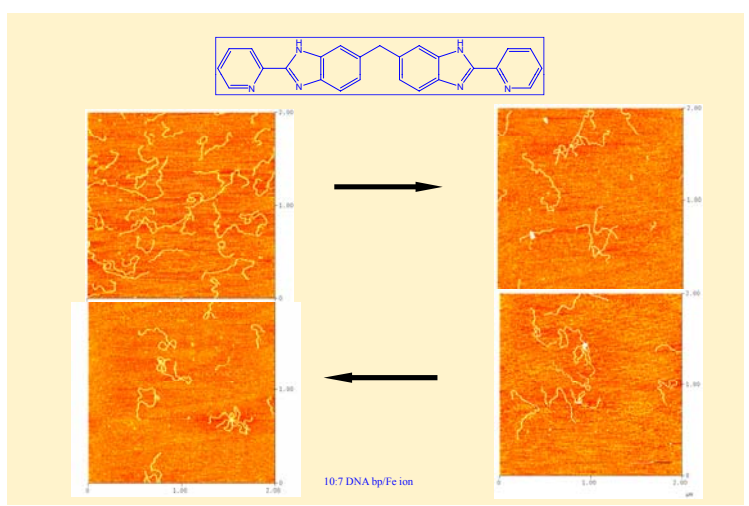
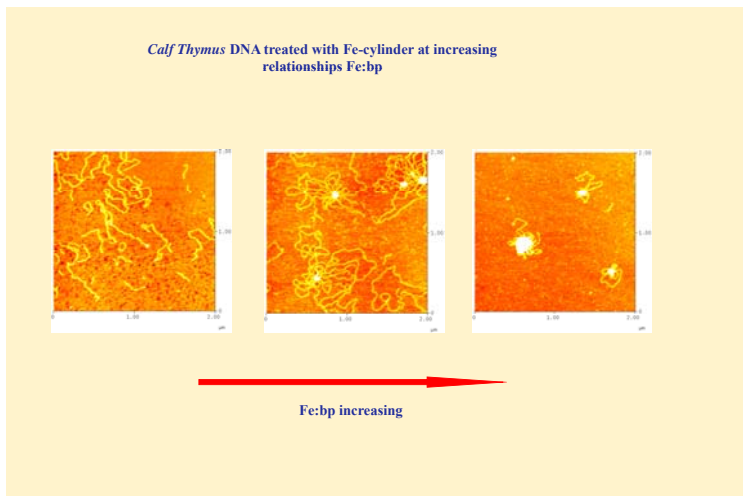
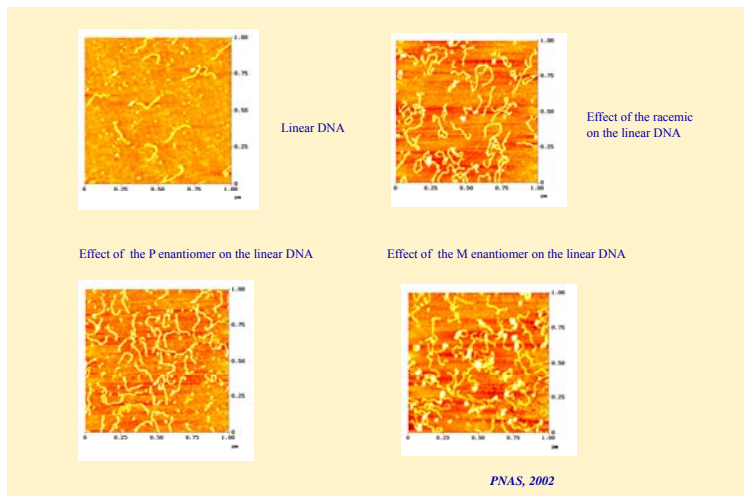
Comparison between a non-treated pBR322 (A), treated with Topoisomerase I (B), and effects of cisplatin (C) and transplatin (D).

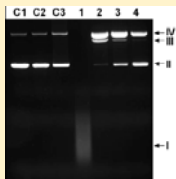
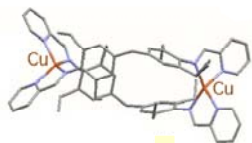


Modifications on linear (left) and plasmid (right) DNA caused by a racemic Co complex

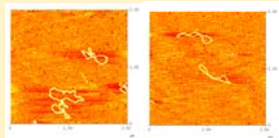
Binding of an iron-supramolecular cylinder to a linear fragment of plasmid DNA







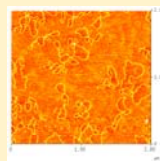
Electrophoresis in agarose gel: pUC19 incubated with $[\text{Cu}_2(\text{L})]^{2+}$ and hydrogen peroxide (HP). Lane C1, free plasmid; lane C2, plasmid with HP. Lane C3, plasmid with $[\text{Cu}_2(\text{L})]^{2+}$ at relationship 10:1 (bp : complex); lanes 1-4, with HP and modified with $[\text{Cu}_2(\text{L})]^{2+}$ at respectively relationships 10:1, 20:1, 40:1 and 100:1. Band I, small fragments of DNA; band II, supercoiled plasmid; band III, linearised plasmid; band IV, relaxed plasmid. $[\text{HP}] = 6.6 \text{ mM}$; $[\text{DNA}] = 250 \text{ }\mu\text{M}$.



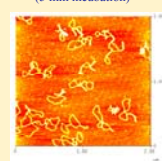
pBR322 DNA with (a) $6 \text{ }\mu\text{M}$ Cu(I) cylinder and (b) $20 \text{ }\mu\text{M}$ Cu(I) cylinder; (c) the same that a) with HP and (d) the same that b) with HP. All samples were incubated for 1 hour at $37 \text{ }^\circ\text{C}$.

Chemistry: A European J., 2006

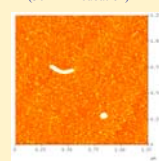
DNA pBR322



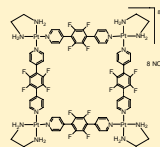
pBR322 + Pt square (5 min incubation)



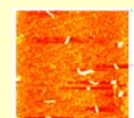
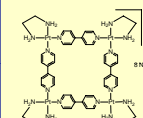
pBR322 + Pt square (30 min incubation)



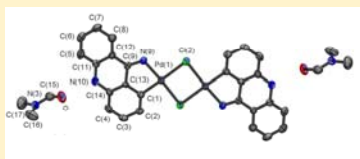
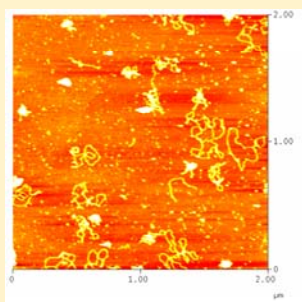
Effect of platinum supramolecular squares on plasmid DNA



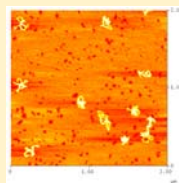
pBR322 + Pt square (same concentration 5 min incubation)



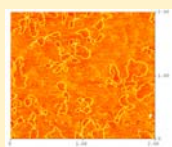
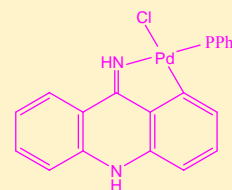
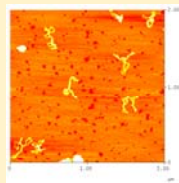
Effect of intercalation in pBR322 plasmid DNA of a di-palladium-9-aminoacridine planar complex



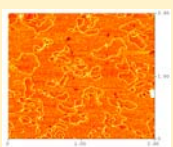
Strong effect on pBR DNA of the mononuclear complex



Palladium probably binds to the N of the bases the intercalation in addition to the intercalation of the acridine molecule



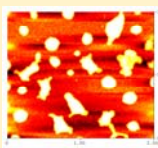
Wild pBR322



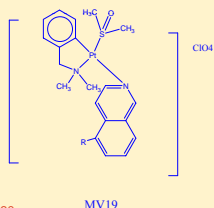
pBR322 with MV19 prepared immediately before imaged (25% diluted)



pBR322 with MV19 imaged after 1 h of incubation (25% diluted)



pBR322 with MV19 imaged after 1 h 30 min of incubation (25% diluted)



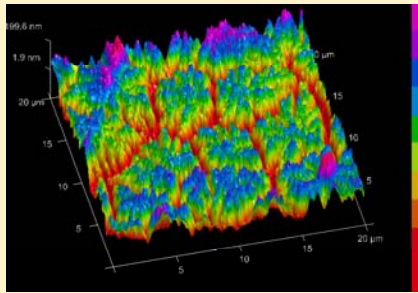
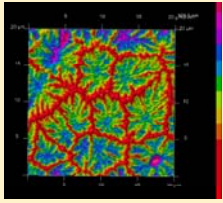
MV19

Spheres were observed using the usual relationship of compound : DNA. By dilution of 25% these images were obtained. Increasing the concentration of compound and/or the time of incubation, the strong interaction of the complex (probably formation of covalent bond by substitution of DMSO molecule by N7 of purine in DNA and intercalation of the planar ligands) produces aggregates forming spheres.

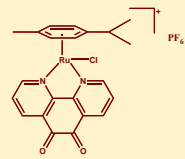
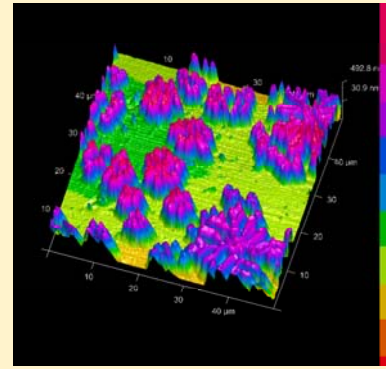
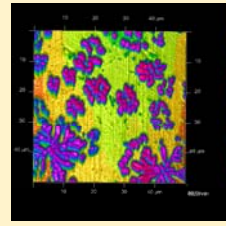
Probing the modifications on cancer processes involved proteins caused by a variety of metal-complexes by Tapping Mode AFM.

The experiments were always done in air, on peeled mica and low humidity.

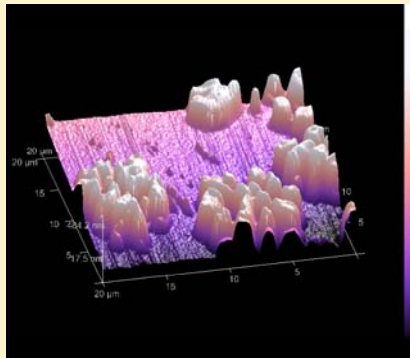
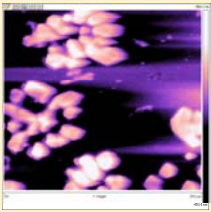
Effect of cytotoxic complexes on fibronectin



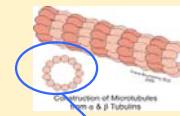
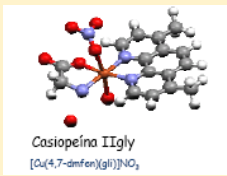
Fibronectin



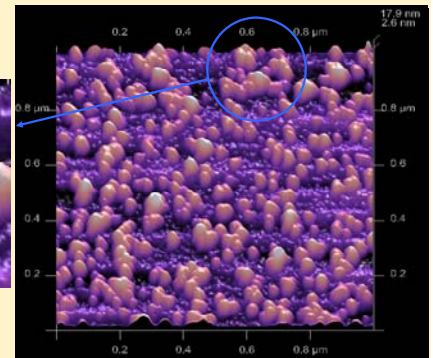
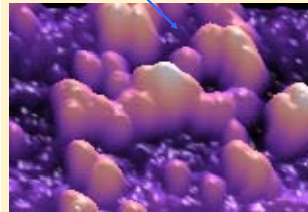
Fibronectin with Ru complex



Fibronectin with Cu complex

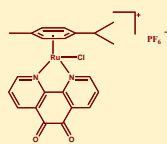
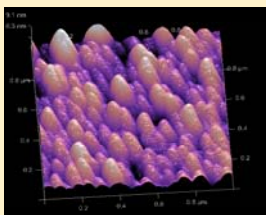
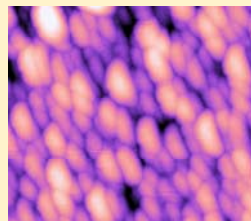


TUBULINE (mica) 1 HOUR 1μm



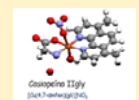
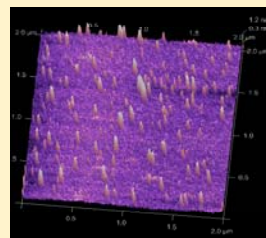
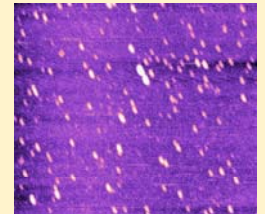
Inhibitor effect of a cytotoxic ruthenium complex on tubuline polymerization

1 HOUR 1μm



Inhibitor effect of a cytotoxic copper complex on tubuline polymerization

1 HOUR 1μm





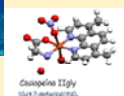
Transferrin

500 nm



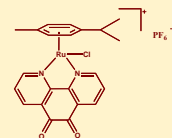
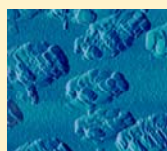
Transferrin-Cu

500 nm



Caspase 12gly
glucosaminoglycans

Effect of cytotoxic complexes on transferrin



Transferrin-Ru

500 nm

CONCLUSIONS

It is possible to image qualitative modifications caused by metal complexes on DNA or proteins

These modifications sometimes are due to formation of covalent bonds between metal ions and heterocycle nitrogen of the purine bases or binding positions of amino acids. In other cases non-covalent interactions (stacking, hydrogen bond, etc.) can be established between the ligands of the metal complexes and phosphate groups, ribose or bases or amino acid chains

Metal ions with possibility of change their oxidation state can break the chains, acting as nucleases. This break can be observed by AFM

Quantitative analysis can be performed by statistical measurement of length, width and height of the forms observed.

Useful information, complementary of other techniques can be obtained by the use of AFM

People involved in the work:

University of Barcelona

Dr. Maria José Prieto
Dr. Bibiana Onoa
Dr. Alberto Martínez
Dr. Marina Gay
Dr. Montserrat Ferrer
Dr. Jordi de Mier
Dr. David Amantia
Dra. GemmamCervantes
Dr. Francesc Xavier Riera
Esther Escribano
Alejandra Rodríguez
Helena Guiset
Ibis Colmenares

Other collaborations:

Prof. Joaquín Borrás (U. Valencia)
Prof. Mike Hannon (U. Birmingham)
Prof. José Ruíz (U. de Murcia)
Prof. Lena Ruíz-Azuara (UNAM)
Dr. Laura Child (U. Warwick)
Dr. Yolanda Parajó (U. de Santiago)
Dr. Juan Jesús Fiol (U. Illes Balears)